

# Optical Droplet Vaporization (ODV): photoacoustic characterization of perfluorocarbon droplets

Eric M. Strohm, Min Rui, Michael C. Kolios

Department of Physics  
Ryerson University  
Toronto, Ontario, Canada  
mkolios@ryerson.ca

Ivan Gorelikov, Naomi Matsuura

Imaging Research Department  
Sunnybrook Health Sciences Centre  
Toronto, Ontario, Canada

**Abstract**— Optical droplet vaporization (ODV) of nanoscale and micron-sized liquid perfluorocarbon (PFC) droplets via a 1064 nm laser is presented. The stability and laser fluence threshold were investigated for PFC compounds with varying boiling points. Using an external optical absorber to facilitate droplet vaporization, it was found that droplets with boiling points at 29°C and 56°C were consistently vaporized upon laser irradiation using a fluence of 0.7 J/cm<sup>2</sup> or greater, while those with higher boiling points did not, up to a maximum laser fluence of 3.8 J/cm<sup>2</sup>. Upon vaporization, the droplet rapidly expanded to approximately 10-20x the original diameter, then slowly and continuously expanded at a rate of up to 1 μm/s. Lead sulphide (PbS) nanoparticles were incorporated into perfluoropentane (PFP) droplets to facilitate vaporization. The fluence threshold to induce vaporization ranged from 0.8 to 1.6 J/cm<sup>2</sup>, the wide range likely due to variances of the PbS concentration within the droplets. Prior to vaporization, the photoacoustic spectral features of individual droplets 2-8 μm in diameter measured at 375 MHz agreed very well with the theoretical prediction using a liquid sphere model. In summary, the use of liquid droplets for photoacoustic imaging and cancer therapy has been demonstrated.

## I. INTRODUCTION

Perfluorocarbon (PFC) droplets are currently being studied as contrast and therapeutic agents for the purpose of cancer imaging and therapy [1]. These droplets contain a liquid PFC core generally encapsulated by a lipid or albumin shell. Liquid PFC droplets have poor ultrasound contrast because of a similar acoustic impedance to surrounding tissue. Vaporization of droplets from liquid to gas phase via ultrasound irradiation has been demonstrated by a method called acoustic droplet vaporization (ADV) [2]. Once vaporized, the ultrasound contrast increases dramatically due to the large acoustic mismatch between the gas core and surrounding tissue. Alternatively, we investigate in this work whether a laser can be used to trigger vaporization using a method we term optical droplet vaporization (ODV).

For imaging and cancer therapy, after intravenous injection, the micron-sized droplets can be vaporized to damage surrounding tissue for targeted drug delivery [3] and vessel occlusion [4]. PFC droplets have advantages over other contrast agents such as microbubbles, as they can be made very small, have a longer half life, are chemically and biologically inert, and appear to be non-toxic to humans [5].

The mechanism of acoustic droplet vaporization is not well understood. While vaporization can occur via inertial cavitation, thermal effects, or a chemical reaction, the thermal mechanism has been suggested as the main mode of vaporization [6]. However, ADV and ODV may have different mechanisms due to the different irradiation sources used for vaporization.

Since PFCs have minimal absorption in the infrared spectrum [7], an optical absorbing material must be incorporated into the droplet to enable ODV. Various materials could be used to facilitate vaporization in PFC droplets using near-infrared lasers, such as gold nanorods, iron oxide, carbon particles, black ink, and lead sulphide (PbS).

The goal of this research is to create a dual-mode contrast agent that can be injected intravenously in liquid form. The PFC droplet size can be either micron-sized (1-5 μm), where the droplet is restricted to vasculature, or nanometer-sized (200 nm), in which the droplets can traverse through the tumor vasculature and accumulate in tumors due to the enhanced permeability and retention effect [8]. The photoacoustic signal from droplets can be measured using an ultrasound probe in passive mode. Once the droplets have reached the targeted area, the laser fluence can be increased to induce ODV. Alternatively, the droplets could be made with materials that absorb at different wavelengths to allow for imaging at one wavelength, and vaporization at the other. The ultrasound probe can also be used to determine the droplet population that was vaporized.

Other studies have mainly concentrated on perfluoropentane (PFP), which has a boiling point (BP) of 29°C. PFP droplets may persist as superheated droplets in liquid form within the body, where surface tension increases the natural boiling point by 40°C [9]. In this study, we probe various PFC compounds with boiling points ranging from 29°C to 174°C using a photoacoustic microscope system to examine the effect of laser fluence and optical absorbing materials on droplet stability and vaporization thresholds. These results will help to understand the vaporization mechanism used in optical droplet vaporization.

## II. THEORY

The photoacoustic response of a liquid sphere when irradiated by a laser with intensity  $I_0$ , as a function of frequency, is given by:

$$p(q) = iAe^{-iq\tau} \frac{(\sin q - q \cos q) / q^2}{(1 - \rho)(\sin q / q) - \cos q + ic\rho \sin q}, \quad (1)$$

$$\text{with} \quad A = \frac{\mu_a \beta c_d I_0 a}{2\pi C_p (r/a)}, \quad (2)$$

where  $a$  is the droplet radius,  $c_d$  and  $c_f$  are the sound velocities in the droplet and coupling fluid, respectively,  $\beta$  is the thermal expansion coefficient,  $C_p$  is the heat capacity,  $\mu_a$  is the absorption coefficient,  $q = 2\pi fa/c_d$  is the dimensionless frequency,  $\tau = (v/a)[t - (r-a)/c_f]$  is the dimensionless delay time from the radius of the droplet, and  $\rho$  and  $c$  are the ratios of the density and sound velocity between the droplet and coupling fluid, respectively [10]. In this study, the constant  $A$  was set to unity as it only affects the amplitude of the signal and does not change the spectral features.

## III. MATERIALS AND METHODS

### A. PFC Emulsions

PbS nanoparticles were synthesized [11], coated with silica [12, 13], and solubilized into PFC [14]. Nanoparticle-incorporated PFC and PFC droplets were prepared using deionized water, nanoparticle-PFC/PFC solution, and an anionic phosphate fluorosurfactant. Nanoscale PFC droplets in water were prepared by sonication, while micron-scale droplets were prepared by membrane emulsification using polymer membranes, following coarse emulsification by vortexing.

PbS nanoparticles were imaged using a Hitachi HD-2000 scanning transmission electron microscope. Nanoscale PFC droplet sizes were measured using a Malvern Zeta-sizer 3000HS (Worcestershire, UK) instrument. Micron-scale PFC droplet size were measured using a Multisizer III Coulter counter (Beckman Coulter Inc., Fullerton, CA).

### B. Photoacoustic Microscope

The SASAM 1000 acoustic microscope (Kibero GmbH, Saarbrücken, Germany), consisting of an Olympus IX81 inverted optical microscope (Olympus, Japan) and an acoustic module for ultrasound measurements, was modified to include a 1064 nm laser (Teem Photonics, France). The laser was collimated through the back port of the microscope and focused by a 10x optical objective onto the sample. Simultaneous laser

irradiation and optical observation via CCD enabled accurate droplet targeting. Details of the system construction can be found elsewhere [15, 16].

An adjustable laser fluence of up to 3.8 J/cm<sup>2</sup> per pulse when focused to a 4  $\mu$ m spot size was possible, using a 10x optical objective with a 0.3 numerical aperture. The laser had a pulse width of 700 ps with a repetition frequency of up to 2 kHz. Acoustic and photoacoustic measurements were made using a transducer with a 375 MHz center frequency, 60° aperture angle and -6 dB bandwidth of 42%. The transducer was used passively during photoacoustic measurements. The signal was amplified by a 40 dB amplifier and digitized at a rate of 8 GHz. For pulse-echo measurements, 10 Vpp pulses were generated at a pulse repetition frequency of 500 kHz, using a monocyte pulse generator with a center frequency of 300 MHz with 100% bandwidth. During photoacoustic measurements, signals were digitized at a rate of 2 kHz, triggered to the laser pulse, and limited by the repetition rate of the laser. 100-200 signals were averaged for each measurement to increase the signal-noise ratio (SNR).

### C. Measurements

All measurements were made at 36°C to simulate physiological conditions within the human body. The effect of PFC boiling point on vaporization thresholds was investigated by depositing droplets 2-5  $\mu$ m in diameter onto a microscope slide. Black ink (Sharpie, USA) was drawn on the microscope slide prior to adding the droplets to simulate laser absorption within the droplet. The laser was focused onto the ink which was directly under a droplet using a laser fluence of 0.7 J/cm<sup>2</sup>. Once vaporization occurred, the microscope slide was refrigerated at 4°C. After 30 minutes, the slide was returned to the microscope and the size of the previously irradiated bubbles was recorded. Four different PFC compounds with boiling points ranging from 29°C to 174°C were examined, as shown in table I.

Below laser thresholds for vaporization, the photoacoustic signal was measured from PFP droplets containing PbS. For the nanoscale droplets, 300 nm diameter droplets in a water suspension were irradiated and the resulting photoacoustic signal recorded. For the micron-scale droplets, droplets of 2-5  $\mu$ m in diameter were deposited on two substrates: a) a glass slide and b) a 50  $\mu$ m thick agar phantom to examine the effects of a droplet at a hard/soft boundary. For both sizes, the laser fluence was gradually increased until vaporization occurred. Immediately after vaporization, ultrasound pulse echo measurements were used to verify a phase change occurred.

TABLE I. LIQUID FLUOROCARBONS

Fluorocarbon	Abbreviation	Structure	Molecular Weight	Boiling Point (°C)	Critical Temperature (°C)	Density (kg/m <sup>3</sup> )	Viscosity (cs)	Sound Velocity (m/s)
Perfluoropentane	PFP	C <sub>5</sub> F <sub>12</sub>	290	29	149	1650	0.4	527
Perfluorohexane	FC72	C <sub>6</sub> F <sub>14</sub>	340	56	176	1680	0.4	468
Perfluoroheptane	FC84	C <sub>7</sub> F <sub>16</sub>	388	80	202	1730	0.55	515
Triperfluorobutylamine	FC43	C <sub>12</sub> F <sub>27</sub> N	670	174	294	1880	2.8	N/A

Perfluorocarbon sound velocity from [7], composition and properties from 3M (St. Paul, MN, USA).

## IV. RESULTS AND DISCUSSION

### A. 300 nm Droplet Vaporization

A suspension of 300 nm diameter PFC droplets containing PbS were irradiated using a 1064 nm with a laser fluence of  $0.5 - 3.5 \text{ J/cm}^2$ . Vaporization was verified by visual inspection. Vaporization was observed at fluences as low as  $0.5 \text{ J/cm}^2$ , and was consistently observed for fluences over  $3 \text{ J/cm}^2$ .

### B. Vaporization and PFC Boiling Point

Using the ink spot as a mechanism to induce ODV on droplets 1-5  $\mu\text{m}$  in diameter resulted in consistent vaporization of PFP (BP =  $29^\circ\text{C}$ ) and FC72 (BP =  $56^\circ\text{C}$ ) droplets. Vaporization of FC84 (BP =  $80^\circ\text{C}$ ) droplets rarely occurred, while FC43 (BP =  $174^\circ\text{C}$ ) never vaporized, even at the maximum laser fluence used in these experiments ( $3.8 \text{ J/cm}^2$ ). A single laser pulse was sufficient to induce vaporization of PFP and FC72 droplets.

Condensation of the PFC vapor back to liquid was investigated. Within a few minutes of ODV, the microscope slide was cooled at  $4^\circ\text{C}$  for 30 minutes. PFP bubbles shrank slightly, however all FC72 bubbles condensed to 1-3  $\mu\text{m}$  diameters. As the temperature increased slowly to  $36^\circ\text{C}$ , some bubbles reformed and expanded. It is unknown why some bubbles expanded upon heating and others did not. It is possible some bubbles were removed during the cooling process, or simply condensed entirely into liquid droplets and became stable again. The bubbles that shrank, but did not disappear may still have had some residual gas left inside, or, there may be some other issue such as contamination from the ink, or a chemical reaction that changed the FC72 composition.

### C. Vaporization Threshold

The photoacoustic signal was measured as a function of laser fluence to examine vaporization thresholds for three droplets containing PbS nanoparticles with diameters 2, 2 and 5  $\mu\text{m}$  using the 375 MHz transducer (fig. 1). The energy at which

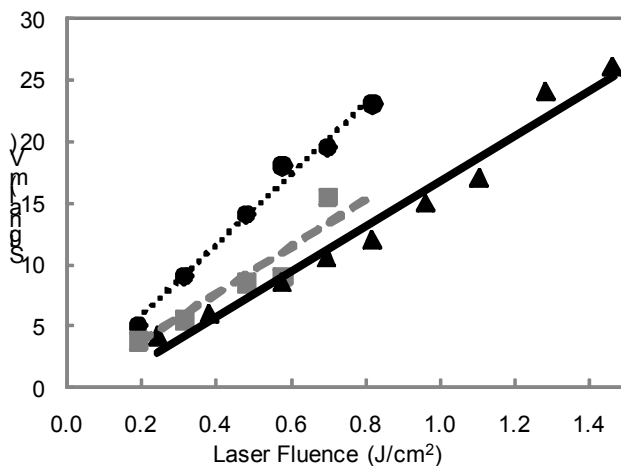


Figure 1. Photoacoustic signal vs. irradiated laser fluence for three droplets with diameters 2  $\mu\text{m}$  (circles and squares), and 5  $\mu\text{m}$  (squares). Threshold for vaporization was 0.8, 1.0 and  $1.6 \text{ J/cm}^2$  respectively.

vaporization occurred was 0.8, 1.0 and  $1.6 \text{ J/cm}^2$ , and the maximum photoacoustic signal measured was 16, 25 and 26 mV. A photoacoustic signal was not detected at the instant vaporization occurred. A possible reason why the vaporization threshold varied could be due to droplet configuration variances, such as shell thickness or PbS nanoparticle concentration. It is unknown how the nanoparticles affect the droplet stability.

### D. Photoacoustic Signals

Droplets 2-5  $\mu\text{m}$  in diameter containing PbS nanoparticles were irradiated with a fluence of  $0.8 \text{ J/cm}^2$  and the photoacoustic signal recorded using the 375 MHz transducer, without inducing vaporization. The measured spectrum from a 5.75  $\mu\text{m}$  droplet and the corresponding theoretical signal using equation 1 is shown in fig. 2. The density and sound velocity used with the theoretical calculations were  $1650 \text{ kg/m}^3$  and 425 m/s. The sound velocity at  $36^\circ\text{C}$  was determined by extrapolating the sound velocity at  $20^\circ\text{C}$  (527 m/s, [6]) using  $-2.67 \text{ m/s/}^\circ\text{C}$  from [17]. Agreement of the spectral features was observed between experiment and theory. The spectra were normalized to maximum amplitude, and were not modified to account for the transducer response or bandwidth. Good agreement was observed with other droplet diameters ranging from 2 to 8  $\mu\text{m}$ .

### E. Vaporization Dynamics

Upon vaporization, bubbles quickly grew to 10-20x their original size (fig. 3), which is consistent with reports of bubble growth during ADV [1]. The bubbles then slowly expanded at a rate of up to 1  $\mu\text{m/s}$ . The initial rapid expansion is likely due to the change in volume upon liquid to gas conversion, and Kripfgans *et al* [1] hypothesized gas diffusion into and out of the bubble was responsible for the change in bubble diameter after the initial expansion. However unlike [1], which observed an eventual decrease in bubble diameter within several minutes, bubbles continuously expanded over time. It is unknown if the difference in growth dynamics between ADV

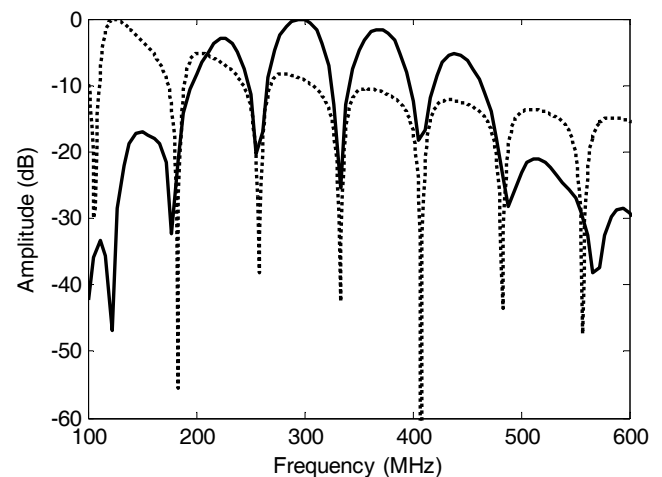


Figure 2. Experimental spectrum (solid line) measured with a 375 MHz transducer and theoretical spectrum (dotted line) using equation 1 with a sound velocity of 425 m/s, density of  $1650 \text{ kg/m}^3$  and 5.75  $\mu\text{m}$  diameter. Results were normalized to maximum amplitude.

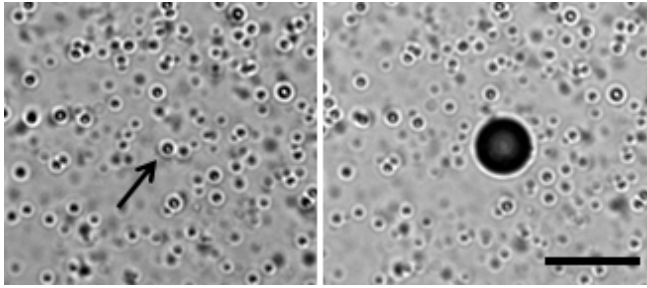


Figure 3. Optical view of a PFP droplet containing PbS before irradiation (left) and immediately after (right). The arrow indicates the irradiated droplet. Scale is 30  $\mu\text{m}$ .

and ODV is due to the irradiation (ultrasound vs. laser), the experimental method or the nature of the emulsion used.

Pulse echo measurements were made before and after laser irradiation. After vaporization, at least a 10x increase in echogenicity was measured from the bubble, indicating a phase change from liquid to gas. Additionally, the ultrasound signal from the substrate, previously detected through the liquid droplet, disappeared after vaporization due to strong attenuation of the gas core. The time of the echo from the bubble surface decreased over time, indicating the height was increasing, which was consistent with the increase in bubble diameter observed optically.

## V. CONCLUSIONS AND FUTURE WORK

This paper presents our initial experiments describing laser-based vaporization of PFC droplets. Future work will examine the effect of different optical absorbers incorporated into the PFC compounds and characterizing these materials using photoacoustic and pulse-echo acoustic microscopy methods. The ultimate goal is to develop a new optically-triggered therapeutic agent for clinical imaging and cancer therapy.

## ACKNOWLEDGMENT

E. Stroh is supported through a NSERC doctoral scholarship. This research was undertaken, in part, thanks to funding from the Canada Research Chairs Program awarded to M. Kolios. Funding to purchase the equipment was provided by the Canada Foundation for Innovation, the Ontario Ministry of Research and Innovation, and Ryerson University. This study was supported, in part, by the CIHR Excellence in Radiation Research for the 21<sup>st</sup> century (EIRR21) Research Training Program, the Ontario Institute for Cancer Research Network through funding provided by the Province of Ontario, the FY07 Department of Defense Breast Cancer Research Program Concept Award (BC075873) and a program project grant entitled "Imaging for Cancer" from the Terry Fox Foundation.

## REFERENCES

- [1] M. L. Fabiilli, K. J. Haworth, I. E. Sebastian, O. D. Kripfgans, P. L. Carson, J. B. Fowlkes, "Delivery of Chlorambucil Using an Acoustically-Triggered Perfluoropentane Emulsion," *Ultrasound Med Biol.*, vol. 36(8), pp. 1364-1375.
- [2] O. B. Kripfgans, J. D. Fowlkes, D. L. Miller, O. P. Eldevik, and P. L. Carson, "Acoustic droplet vaporization for therapeutic and diagnostic applications," *Ultrasound Med Biol.*, vol. 26, 2000, pp. 1177-1189.
- [3] G. M. Lanza and S. A. Wickline, "Targeted ultrasonic contrast agents for molecular imaging and therapy," *Progress in cardiovascular diseases*, vol. 44, 2001, pp. 13-31.
- [4] O. Kripfgans, J. Fowlkes, M. Woydt, O. P. Eldevik, and P. L. Carson, "In vivo droplet vaporization for occlusion therapy and phase aberration correction," *IEEE transactions on Ultrasonics, Ferroelectrics and Frequency Control*, vol. 49(6), 2002, pp. 726-38.
- [5] C. S. Cohn and M. M. Cushing, "Oxygen therapeutics: perfluorocarbons and blood substitute safety," *Critical care clinics*, vol. 25, 2009, pp. 399-414.
- [6] K. C. Schad and K. Hynynen, "In vitro characterization of perfluorocarbon droplets for focused ultrasound therapy," *Physics in medicine and biology*, vol. 55, 2010, pp. 4933-47.
- [7] W. L. Hasi, Z. W. Lu, S. Gong, S. J. Liu, Q. Li, and W. M. He, "Investigation of stimulated Brillouin scattering media perfluorocompound and perfluoropolyether with a low absorption coefficient and high power-load ability," *Applied optics*, vol. 47, 2008, pp. 1010-4.
- [8] S. K. Hobbs, W. L. Monsky, F. Yuan W. G. Roberts, L. Griffith, V. P. Torchilin, R. K. Jain, "Regulation of transport pathways in tumor vessels: role of tumor type and microenvironment," *Proc Natl Acad Sci USA*, vol. 95(8), pp. 4607-12.
- [9] T. Giesecke and K. Hynynen, "Ultrasound-mediated cavitation thresholds of liquid perfluorocarbon droplets in vitro," *Ultrasound Med Biol.*, vol. 29, 2003, pp. 1359-1365.
- [10] M. I. Khan and G. J. Diebold, "The photoacoustic effect generated by an isotropic solid sphere", *Ultrasonics*, vol. 33(4), 1995, pp. 265-269.
- [11] M. A. Hines and G. D. Scholes, "Colloidal PbS nanocrystals with size-tunable near-infrared emission: Observation of post-synthesis self-narrowing of the particle size distribution," *Advanced Materials*, 2003, 15(21) pp. 1844-1849.
- [12] I. Gorelikov, N. Matsuura, "Single-step coating of mesoporous silica on cetyltrimethyl ammonium bromide-capped nanoparticles", *Nano Lett.*, 8 (2008) 369-373.
- [13] D. K. Yi, S. T. Selvan, S. S. Lee, G. C. Papaefthymiou, D. Kundaliya, J. Y. Ying, "Silica-coated nanocomposites of magnetic nanoparticles and quantum dots," *J. Am. Chem. Soc.*, 127 (2005) 4990-4991.
- [14] N. Matsuura, et al., "Nanoparticle-Tagged Perfluorocarbon Droplets for Medical Imaging," in *Advances in Material Design for Regenerative Medicine, Drug Delivery and Targeting/Imaging*, V.P. Shastri, et al., Editors. 2009. p. 87-92.
- [15] M. Rui, S. Narashimhan, W. Bost, F. Stracke, E. Weiss, R. Lemor, and M.C. Kolios, "Gigahertz optoacoustic imaging for cellular imaging," *Proc. SPIE*, vol. 7564, 2010, p. 756411.
- [16] W. Bost, F. Stracke, E. C. Weiss, S. Narashimhan, M. C. Kolios, and R. Lemor, "High frequency optoacoustic microscopy," *Annual International Conference of the IEEE Engineering in Medicine and Biology Society*, 2009, pp. 5883-6.
- [17] J. N. Marsh, C. S. Hall, S. A. Wickline, G. M. Lanza, "Temperature dependence of acoustic impedance for specific fluorocarbon liquids," *J Acoust Soc Am.*, 12(6), 2002, pp. 2858-62.